Materials Research Proceedings 41 (2024) 2584-2594 https://doi.org/10.21741/9781644903131-284

Optimization of the temperature profile of PET preform via a 3D modelling of the Infrared Heating and ventilation

LUO Yun-Mei[1,a*], CHEVALIER Luc[1,b], NGUYEN Thanh Tung[1,c]

[1]Université Gustave Eiffel, Laboratoire Modélisation et Simulation Multi Echelle, MSME UMR 8208 CNRS, 5 bd Descartes, 77545 Marne-la-Vallée, France

[a]yun-mei.luo@univ-eiffel.fr, [b]luc.chevalier@univ-eiffel.fr, [c]thanh-tung.nguyen@univ-eiffel.fr

Keywords: Infrared Heating, Numerical Simulation, Ventilation Effect, Optimization

Abstract. Thermal effect has important influence during the stretch blow moulding (SBM) process of PET bottle. Setting the heating condition in an industrial context is a complex task. A 3D simplified modelling of the heating stage during this process is proposed. In this numerical approach, the radiation source is simulated by using a model for intensity of the incident radiation and the Beer Lambert's law. On the other hand, the ventilation effect under industrial condition is taken into account by a modelling of the forced convection around a cylinder. The IR flux and ventilation effects are implemented as thermal boundary conditions in COMSOL for a 3D computation of the thermal problem for the preform only. Based on this simplified approach to achieve quickly the numerical simulation of the preform heating, an optimization procedure is proposed to adjust the settings of the infrared lamps by comparing our simulation results to the target temperature profile. This optimization tool provides quickly a first set of parameters to help industrial to obtain the desired temperature profile.

Introduction

The stretch blow moulding (SBM) process is a manufacturing process which is widely used to produce the plastic bottles and containers. In this process, a tube like preform is heated in front of infrared (IR) lamps, stretched, and then blown into the desired bottle shape within a mold. There have been numerous researches on the experimental approach and on the numerical one over the last 30 years [1-7]. However, the performance requirements of material PET and of the final bottle regularly increase, that leads to an upgraded investigation on the thermal and mechanical response of the process.

The temperature distribution of the preform before the blowing stage and thermal effect have important influence during the SBM process of PET bottle [8-10]. They plays an important role in the final thickness distribution and induced properties [11]. Numerous works have been carried out to obtain accurately the temperature distribution of the heating stage and to improve the design of infrared-ovens [11-13]. In author's previous works [10,14], the thermal properties of PET have been firstly identified from injected sheet. The IR heating flux was calculated by using radiative laws adapted to the test geometry in a semi-analytic way. For the preform case, the radiation source is simulated by using same model for intensity of the incident radiation and the Beer Lambert's law. On the other hand, in order to simulate a more realistic ventilation effect under industrial condition, we consider a simplified modelling of forced convection. The IR flux and ventilation effects are implemented as thermal boundary conditions in COMSOL for a 3D computation of the thermal problem for the preform only. The numerical temperature distribution of the external surface of the preform is compared to the measured internal and external temperature of preforms from THERMOscan device [15] in order to validate the approach. This device is provided by Blow Moulding Technologies Ltd. (BMT) company in Belfast. It measures simultaneously the internal and external preform temperature profile.

The objective of this paper is to provide an optimization procedure in order to adjust the settings of the heating steps by comparing our simulation results to the temperature profile target.

The simulation from the simplified modelling takes only a few minutes and is the elementary brick of the optimization procedure. The study of the elementary contribution of each lamp on the temperature distribution in different regions of the preform is carried out. On the other hand, the effect of the accumulation of sub-steps on the temperature distribution of the preform is also studied. Based on the results of the elementary increase of temperature for each lamp and the target temperature, a system of linear equations related to the three different regions (bottom, middle and neck) can be written. The optimization procedure can be achieved by minimizing the residual of the three equations using different setting of lamps on each sub-step.

Heating system presentation

Figure 1 presents the heating system including two series of ten infrared lamps. A preform transport chain including a rotation system for the preforms to turn around their axis when passing in front of the lamps, reflectors on the opposed side of the lamps to provide a radiative flux on the rear part of the preforms and a ventilation system composed of three fan turbines is used to cool the neck of the preform to make sure it does not deforms during the blowing process. It also helps to regulate the temperature in the thickness of the preform.

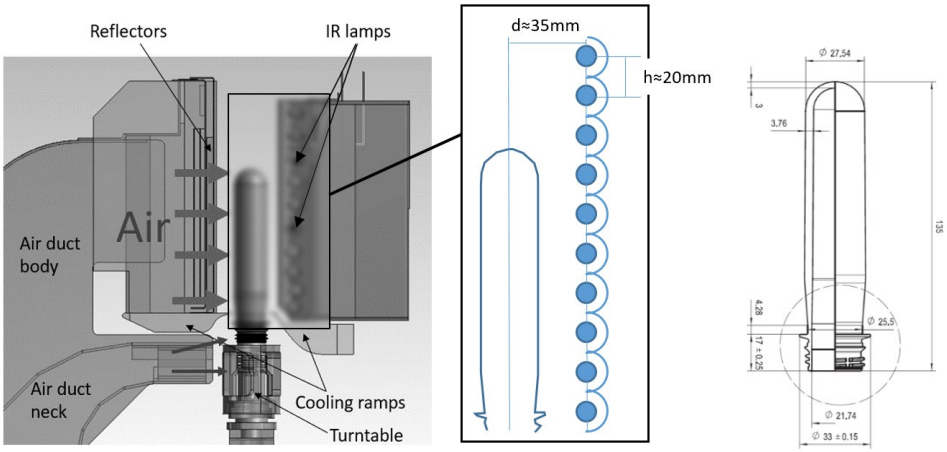

Figure 1: The heating system presentation with architecture of lamps and preform. The figure is partially blurred for confidentiality reasons [14].

One can control the power of each IR lamp to obtain a required temperature distribution in the height of the preform. Figure 2 shows the four steps and eight sub-steps of the heating stage:

(i) from 0 to 6s the preform is heated through the first set of IR lamps and ventilation;

(ii) from 6 to 19s, air stabilization step to reduce the difference between the outside and the inside temperature of the preform;

(iii) from 19 to 25s, the preform is heated again through the second set of lamps;

(iv) from 25 to 38s the preform is transferred in the mold.

The duration of the two heating steps (i) and (iii) is 6s each. Three sets of lamps are to be adjusted for each step, the preform passes 2s in front of each set. Consequently, in order to obtain the best temperature profile, the 8 lamps have to be turned on or off during the 6 sub-steps of 2s each. With the 2 air stabilization step, one highlights 8 sub-steps in the Fig. 2.

During the first step, the temperature of the outside of the preform is more important than the inside one. During the second step, the temperature of the external surface decreases while the internal temperature keeps rising by conduction from the outside. Therefore, the temperature becomes more homogeneous in the thickness during this step. After the IR heating of the third step, the difference of temperature through the thickness increases again. The last step is a second

homogenization period for the temperature to become uniform through the thickness while the preform is transported from the oven to the mold. One must notice that for this specific preform, only 8 lamps (from 1 to 8) are used. The target temperature profile is given in Fig.3. This is the average temperature between the external and the internal one which is provide by Sidel group. One can notice that the target temperature is only given from just under the neck to the bottom of the preform. To preserve the cap the temperature must be under 50°C and the air duct neck addresses this. The mid height of the preform needs to be less heated than the top or bottom regions: this is necessary to obtain the best thickness distribution after blowing.

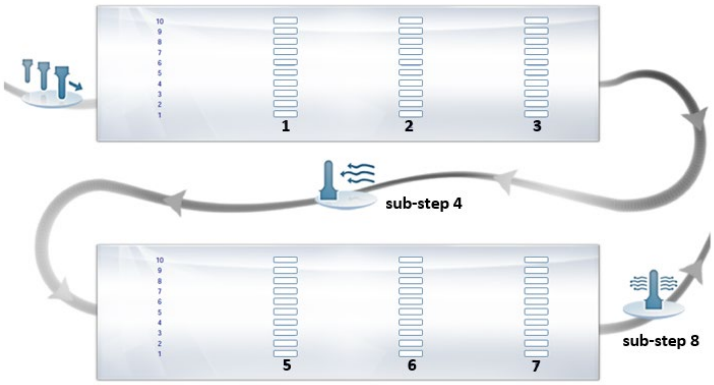

Figure 2: The path of the preform in the heating oven. 3 heating sub-steps followed by an homogenization step and then 3 more heating sub-steps and a final homogenization step before stretching and blowing [14]

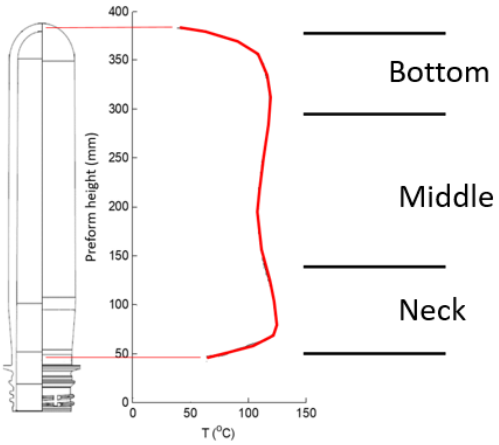

Figure 3: Target temperature profile

IR heating and ventilation

In previous work of authors [10,14], we developed a simplified method to calculate the IR heating flux. A quasi-analytical model is performed to quantify the intensity of the incident radiation. This model together with Beer Lambert's law, can simulate the radiation source term in the heating equation. The model has been used here to characterize the contribution of each of the 8 lamps as shown in Fig. 4. Table 1 gives the characteristics of the lamps used for the simulation. The IR radiation flux is calculated on cylindrical coordinates (r,θ,z) on the preform surface and interpolated by an exponential function where coefficient *a* to *f* are determined for each lamp contribution. Table 2 summarizes the 8 sets of identified values of the coefficients in Eq.1a.

$$q_{flux} = a\exp\left(b\theta^2 + c\theta + dz^2 + ez + f\right) \quad (1a)$$

Considering the geometry of preform, the intensity of internal radiation is considered as one-dimensional (through thickness) and quantified by Beer Lambert's law. For the preform case, one can adapt to the geometry as follows:

$$\overrightarrow{q_r} = q_{flux} e^{-k_\lambda (R-r)} \left(-\overrightarrow{e_r}\right) \tag{1b}$$

This can lead to the source term that writes:

$$div\left(\overrightarrow{q_r}\right) = \frac{\partial u}{\partial r} + \frac{u}{r} = -k_\lambda q_{flux} e^{-k_\lambda (R-r)} + \frac{q_{flux} e^{-k_\lambda (R-r)}}{r}$$
$$\Rightarrow div\left(\overrightarrow{q_r}\right) = \left(\frac{1}{r} - k_\lambda\right) q_{flux} e^{-k_\lambda (R-r)} \tag{1c}$$

where r is the classic current radius, R is external radius and k_λ is the spectral absorption coefficient for the PET material. The absorption is maximum for the wavelength between 5 and 15 µm and varies from 1.10^4 – 7.10^4 m^{-1}. Here, we choose 3.10^4 m^{-1}. There is no influence on the simulation since k_λ is above 500m-1: the value of this parameter has no much influence on the result. The expression of Eq. 1c will be considered in the heat equation for the simulation in the following.

Table 1: Different heating characteristics

T of filament (K)	Number of lamps and global height	Distance between lamps and preform	Length of lamps
2700	8 lamps 172.5 mm	30 mm	306 mm

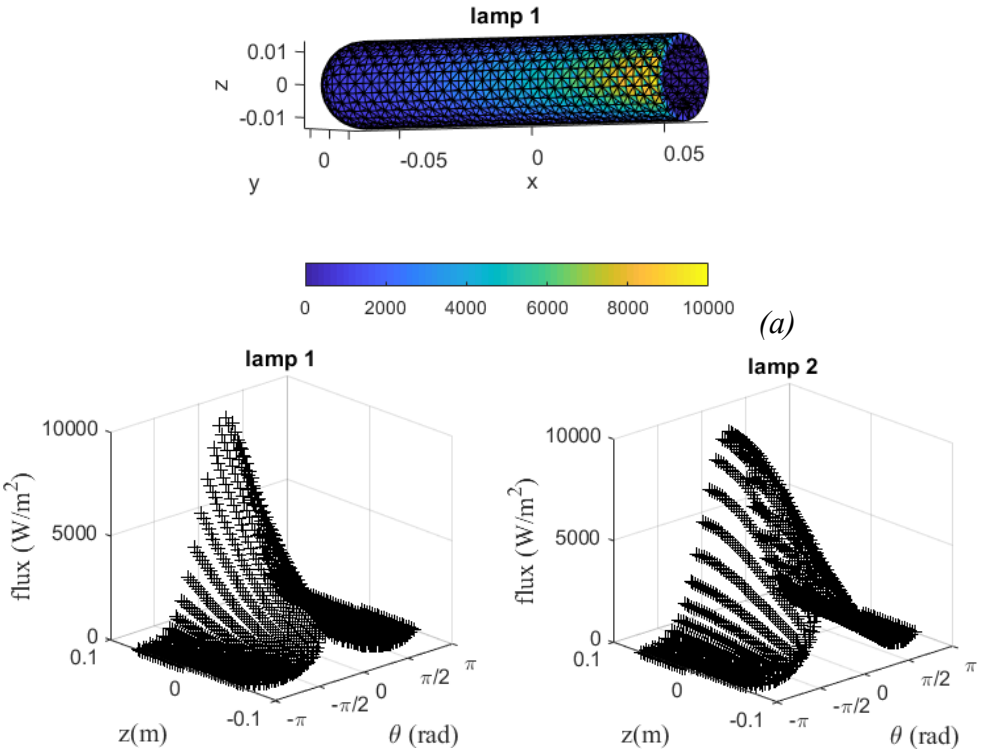

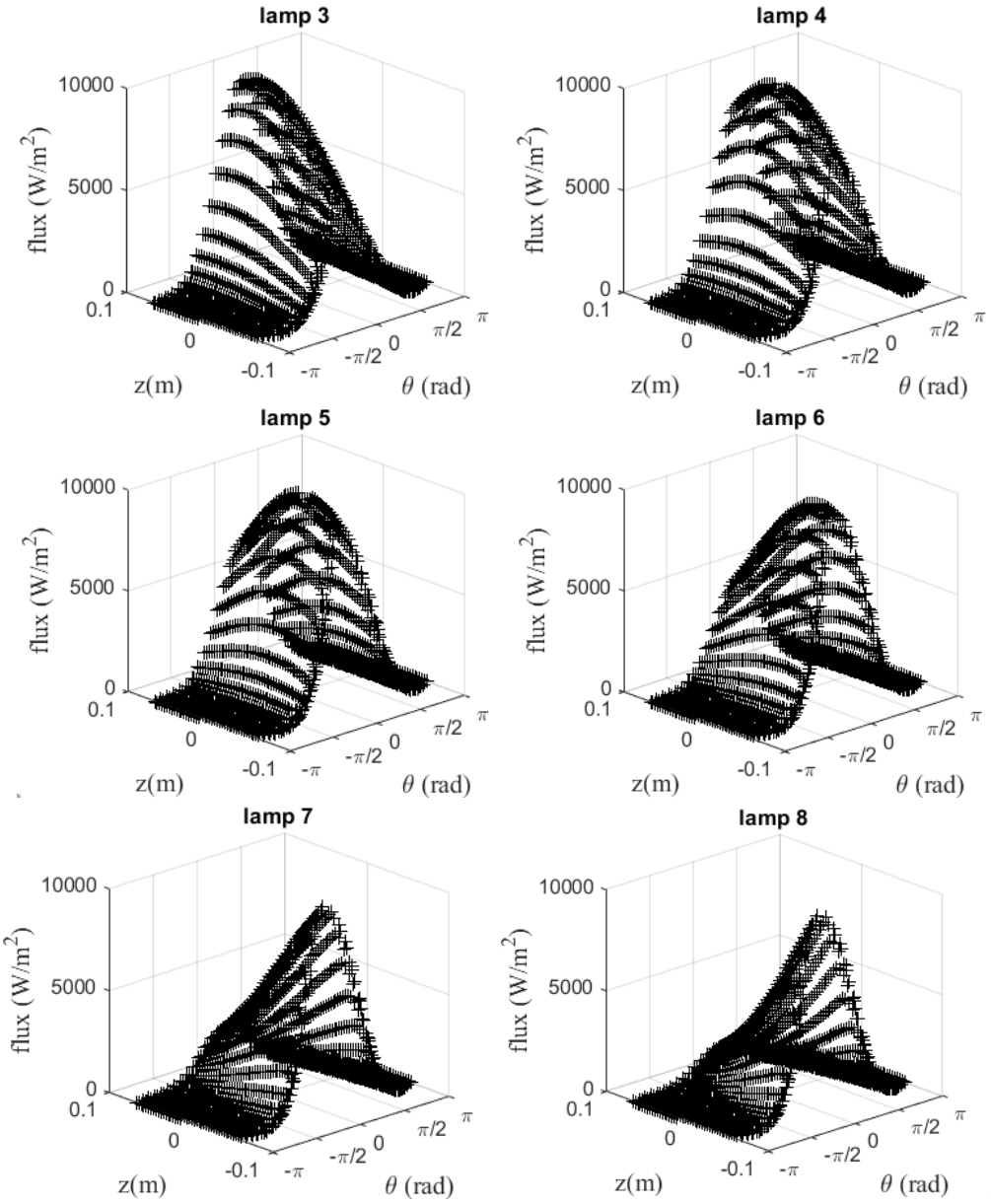

(b)

Figure 4:: (a) IR radiation flux calculated preform from lamp 1; (b) interpolated function of z and θ for each lamp

Table 2 : Identified values of the coefficients in Eq. 1 for each lamp with θ expressed in rad and z in mm

	Lamp 1	Lamp 2	Lamp 3	Lamp 4	Lamp 5	Lamp 6	Lamp 7	Lamp 8
a *(W/m²)*	1.487	10.286	12.808	11.805	12.553	12.086	2.154	1.693
b	-0.719	-0.702	-0.723	-0.74	-0.757	-0.771	-0.772	-0.772
c	-0.0138	-0.0025	-0.0058	-0.0082	-0.0103	-0.117	-0.0202	-0.0112
d(m⁻²)	-50.45	-64.09	-64.67	-66.9	-72.5	-68.46	-56.19	-60.19
e(m⁻¹)	19.28	8.68	5.364	1.864	-1.737	-5.265	-11.62	–15.62
f	7.735	6.534	6.534	6.732	6.674	6.609	7.89	7.99

Optimization procedure

For the convective exchange with the airflow around the preform, we considered a simple model by consuming the preform as a cylinder [14]. Based on the IR flux and the air convection coming from the ventilation as two turning boundary conditions, one can manage fast thermal simulation with Comsol. The 3D thermal simulation of PET preform using finite element method is carried out with the following characteristics:

- Thermal conductivity of PET: k = 0.4 (W/m.K)
- Density of PET: ρ= 1.20 (g/(cm^3))
- Heat capacity: $C_p = \Delta C_p \arctan\left(\alpha\left(T - T_g\right)\right) + C_{p1}$ with $\Delta C_p = 220 J/kg.K, \alpha = 0.1, T_g = 87°C, C_{p1} = 1400 J/kg.K$
- h is the exchange convection parameter that is related to the Nusselt number by: $Nu = \frac{hL_c}{k}$

with k the thermal conductivity of the air and L_c a characteristic length of the preform. The ventilation system leads to the air velocity that is near 8m/s when blowing on the neck, and only 1.3m/s in the cylindrical region of the preform. Consequently we can estimate the Reynolds number Re = 2800 for this case. The Nusselt number can be extrapolated from Re.

In order to get the target temperature (Fig. 3), at first, a simulation is managed with the 8 lamps turned on to test the order of magnitude of the increase of temperature. Four situations are considered: lamps on at sub-step 3 only, at sub-step 7 only (these two are chosen because they are followed by a homogenization step), at sub-step 3 and 7 together and finally at sub-step 3, 6 and 7 together. In all four cases, the initial temperature is 30°C on the entire preform and the final temperature profile is almost uniform. The mean increases of temperature are respectively: 32°C, 33°C, 60°C and 82°C. It is to be noticed that for the last case (3, 6 and 7 turned on) the final mean temperature is equal to 82+30=112°C that is too high for the central zone target. We can observe that the increase of temperature is more or less 30°C for each supplementary series of lamps. Considering this semi additivity of the lamp contribution, one is interested to study the contribution of each lamp.

Under the condition which sub-steps 3 and 7 are turned on all the 8 lamps, it remains 35°C near the bottom and almost 30°C near the neck of the preform to increase in order to obtain the target temperature. It remains only 4 lines and 8 lamps: 32 calculations. We define three indicators that are the mean temperature near the bottom of the preform, in the middle region and near the top. For each case, a simulation is carried out and Fig.5 summarizes the final temperature for the three regions. One can see that: (i) the sub-step has a very small influence on the final temperature ; (ii) lamps on position 6, 7, 8 have the highest contribution near the bottom, while lamps 4, 5 and 6 have contribution in the middle, because of the boundary condition, the contribution is not so clear for lamp 1, 2 and 3 ; (iii) elementary contribution of each lamp never exceed 4°C. Because of observation (i) we will consider, in the following, the mean increase of temperature illustrated by the red line in Fig.5. The numerical values of the elementary increase of temperature are given in Table 3.

Table 3 : Mean influence of each lamp on the different region of the preform

Lamp position	8	7	6	5	4	3	2	1
Mean increase of T bottom (°C)	3.694	3.432	2.898	3.097	2.742	0.8	0.727	0.649
Mean increase of T middle (°C)	2.154	2.218	2.155	3.222	3.275	1.575	1.658	1.681
Mean increase of T neck (°C)	0.764	0.965	1.118	2.494	3.045	2.63	3.247	3.651

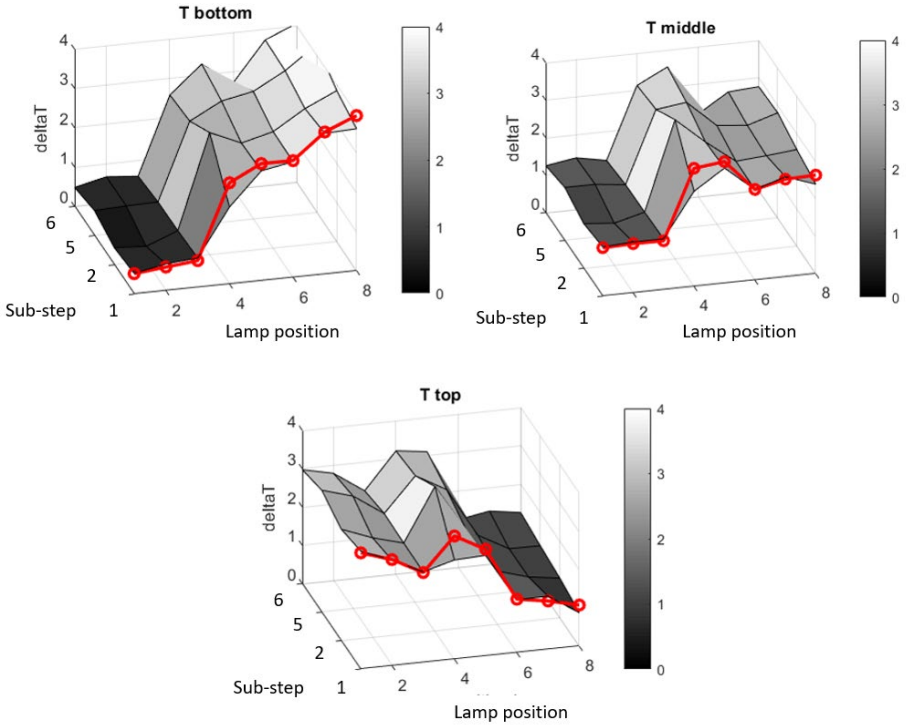

Figure 5. Contribution of each lamp: increase of temperature in °C as a function of the lamp number and the sub-step when the lamp is turned on

The last series of calculations focus on the effect of the accumulation of sub-steps. For each lamp, we simulate the heating of the preform when it is turned on during sub-step 1, then 1 and 2 then 1, 2, 5 and finally 1, 2, 5 and 6: totally 8X3 =24 calculations.

Figure 6 summarizes the results of these simulations. One can observe the quasi-linearity of the accumulation. For example, if lamp 8 is only turned on during sub-step 1, the increase of temperature is 3.6°C, when the same lamp is turned on in the four sub-steps 1, 2, 5 and 6, the increase is 14.5°C that is almost equal 4 times 3.6.

Thanks to the quasi-linearity of the accumulation, we propose the following method to set the entire lamps. First, we evaluate the difference between the preliminary calculation when the 8 lamps are turned on during sub-steps 3 and 7 and the target temperature in each zone. It appears that 32.2°C are needed in the bottom region, 29.1°C in the neck region and only 23.9°C in the middle one as shown in Table 4.

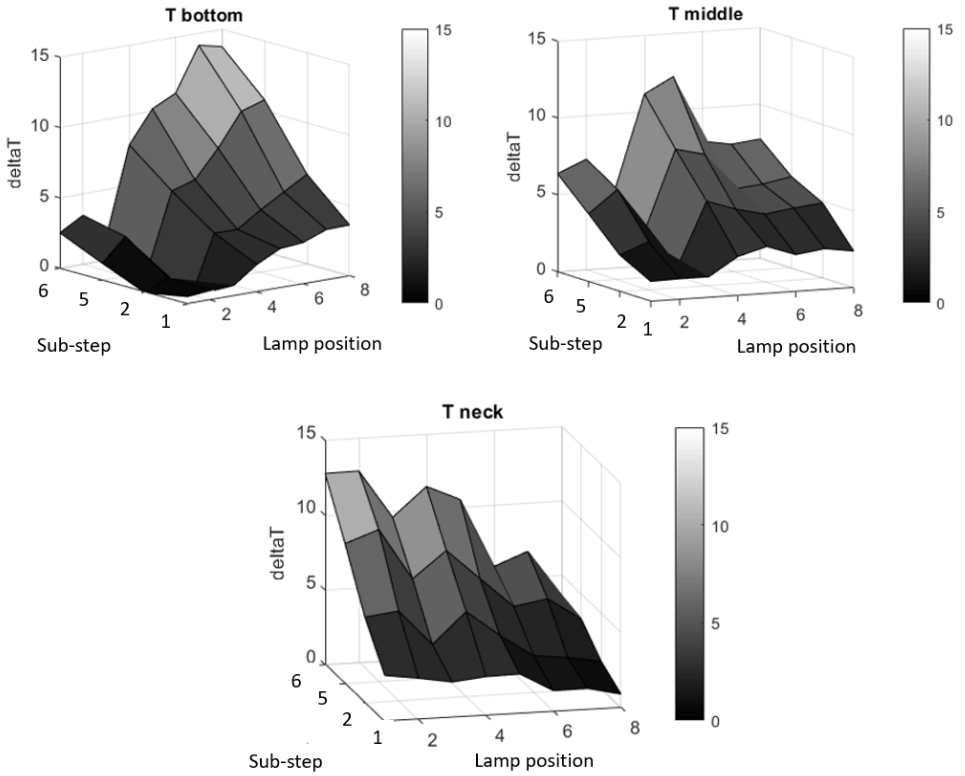

Figure 6. Effect of the accumulation of sub-steps for each lamp on the final temperature

Table 4. Increase of temperature needed in the three regions of the preform

	T mean Zone bottom (°C)	T mean Zone middle (°C)	T mean Zone neck (°C)
Numerical simulation with 8 lamps at sub-steps 3 and 7	89.35	88.74	90.03
Target temperatures on the 3 regions	121.35	112.54	119.83
Increase of temperature needed	32.0	23.8	29.8

We consider the indicator Xi where i is the number of the lamp and that can equal to 1, 2, 3 or 4 when the lamp i is on, respectively in one to four sub-steps. Xi is equal to 0 when the lamp is off. It is then possible to take advantage of the quasi linearity to write the following system based on results of Tables 3 and 4:

$$\begin{aligned} &3.694X_8+3.4318X_7+2.898X_6+3.097X_5+2.742X_4+0.8X_3+0.727X_2+0.649X_1=32.0\\ &2.1541X_8+2.218X_7+2.1545X_6+3.222X_5+3.275X_4+1.575X_3+1.658X_2+1.681X_1=23.8\\ &0.7635X_8+0.965X_7+1.118X_6+2.494X_5+3.045X_4+2.630X_3+3.247X_2+3.651X_1=29.8 \end{aligned} \quad (2)$$

Because each of the 8 indicators Xi can take 5 integer values, this leads to 58 possibilities for the Xi. It is very fast to compute the 390 625 cases and to look at the residual difference defined by Eq.3 where the 3 functions are the left hand terms of Eq.2:

$$error=\left|f_{bottom}(X_i)-32.0\right|+\left|f_{middle}(X_i)-23.8\right|+\left|f_{neck}(X_i)-29.8\right| \quad (3)$$

Table 5 gives the optimized choice of each lamp for the entire 8 sub-steps.

Table 5. The optimal lamps configuration for the target temperature profile.

	Lamp →	**8**	**7**	**6**	**5**	**4**	**3**	**2**	**1**
Sub-step 1	0-2s	X							
Sub-step 2	2-4s	X	X					X	X
Sub-step 3	4-6s	X	X	X	X	X	X	X	X
Sub-step 4	6-19s	Stabilization							
Sub-step 5	19-21s	X	X			X		X	X
Sub-step 6	21-23s	X	X					X	X
Sub-step 7	23-25s	X	X	X	X	X	X	X	X
Sub-step 8	25-38s	Stabilization							

Figure 7 compares this prediction with the target. One can see that the prediction is very good for the bottom region where the temperature is 3°C lower than the target. In the middle region, the prediction is 2°C higher than the target and the neck region is the quite good except the curvature that cannot be simulated correctly because of the boundary condition in the finite element simulation. That leads to the mean temperature in this region about 1°C higher than the target. To provide a better simulation in this region, one should also simulate the screw of the preform. Furthermore, if one divides the preform in more regions, the simulations and the optimization could be more accurate. This would not lead to more finite element simulations, the only difference would more relations to satisfy in Eq.2 and this would not take a higher CPU time.

Figure 8 presents the temperature evolution over time for the three different zones. The red curves show the temperature evolution of the outside surface: the temperature increases in sub-steps 1, 2, 3 and 5, 6, 7, decreases in sub-steps 4 and 8. The blue curves show the evolution of temperature of the inside surface of the preform. This last increases during the whole heating stage because of the thermal conduction that homogenizes the temperature in the thickness during the sub-steps 4 and 8.

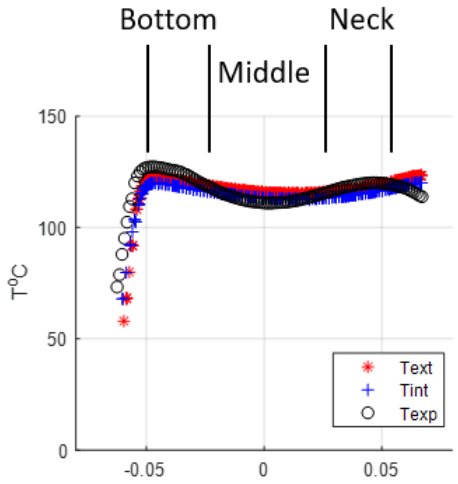

Figure 7. Comparison of the best final temperature (red and blue) with the target profile

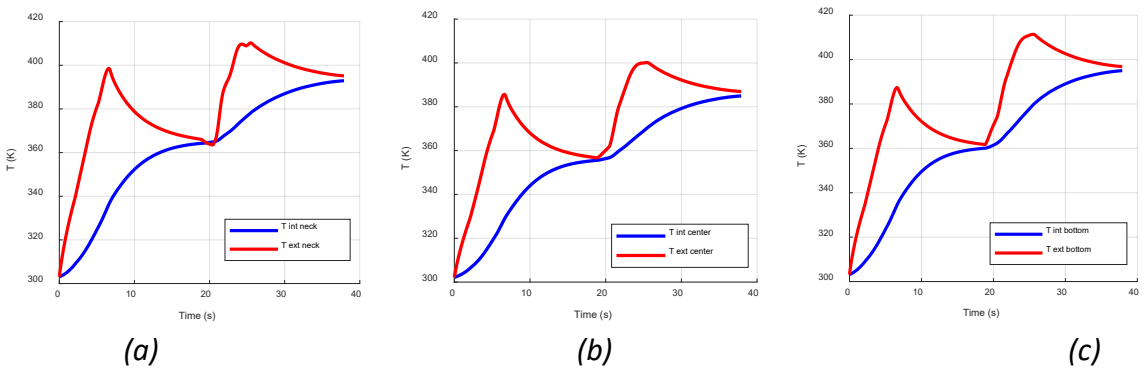

Figure 8. Temperature evolution (a) in the neck zone; (b) in the middle zone; (c) in the bottom zone

Conclusion and discussion

A simplified modelling of the heating stage during SBM process under the industrial condition has been proposed and managed in our previous work. This simulation takes only a few minutes and is the elementary brick of the optimization procedure. In this study, eight lamps are chosen to heat the preform. The heating system involves three heating sub-steps followed by an homogenization step and then three more heating sub-steps and a final homogenization step before stretching and blowing.

In the numerical simulation, the intensity of the incident radiation for each lamp is calculated by a quasi-analytical model. The study of the elementary contribution of each lamp on the temperature distribution in the bottom, middle and neck region of the preform is carried out. Thanks to the low thermal conductivity of the PET, effect of each lamp remains localized in the area of the height of the lamp. The mean influence of each lamp on the different region of the preform is obtained. On the other hand, the effect of the accumulation of sub-steps on the temperature distribution of the preform is almost linear.

Based on the results of the elementary increase of temperature for each lamp and the target temperature, three linear equations related to the three different regions (bottom, middle and neck) can be written. The optimization procedure can be achieved by minimizing the residual of the three equations using different integer values Xi related with the number of sub-steps where the lamps are turned on or off. This optimization tool allows to get quickly a first set of heating lamps, with a good representation of the target temperature.

Acknowledgement

The authors thank Sidel group that provided measurements during the blow moulding process.

References

[1] Luo Y.-M., Chevalier L. On induced properties and self heating during free blowing of PET preform. (2019) International Polymer Processing, 34 (3), p. 330 - 338. https://doi.org/10.3139/217.3759

[2] G.H. Menary, C.G. Armstrong, R.J. Crawford, J.P. McEvoy. (2000). Modelling of poly(ethylene terephthalate) in injection stretch–blow moulding, Plastics, Rubber and Composites, 29:7, 360-370. https://doi.org/10.1179/146580100101541166

[3] N. Billon, M. Picard, E. Gorlier. (2014). Stretch blow moulding of PET; structure development and constitutive model. Int J Mater Form 7, 369–378. https://doi.org/10.1007/s12289-013-1131-1

[4] F.M. Schmidt, J.F. Agassant, M. Bellet. (1998). Experimental study and numerical simulation of the injection stretch/blow molding process. Polym Eng Sci, 38: 1399-1412. https://doi.org/10.1002/pen.10310

[5] Luo Y.-M., Chevalier L., Monteiro E., Utheza F. Numerical simulation of self heating during stretch blow moulding of PET: viscohyperelastic modelling versus experimental results (2021) International Journal of Material Forming, 14 (4), p. 703 - 714, 10.1007/s12289-020-01565-w

[6] Timur, M. The Effect of Temperature, Pressure and Stretch Bar on Product Quality in Production of 0.5 L Pet Bottle. Int. J. Precis. Eng. Manuf. (2023). https://doi.org/10.1007/s12541-023-00899-0

[7] H. Groot, C.G. Giannopapa, R.M.M. Mattheij. A Computer Simulation Model for the Stretch Blow Moulding Process of Polymer Containers. Proceedings of the ASME 2010 Pressure Vessels and Piping Division/K-PVP Conference. ASME 2010 Pressure Vessels and Piping Conference: Volume 5. Bellevue, Washington, USA. July 18–22, 2010. pp. 567-576. ASME. https://doi.org/10.1115/PVP2010-25710

[8] Y.M. Luo, L. Chevalier, F. Utheza. X. Nicolas. Simplified Modelling of the Infrared Heating Involving the Air Convection Effect before the Injection Stretch Blowing Moulding of PET Preform. Material Forming ESAFORM 2014, May 2014, Espoo, Finland. Jari Larkiola, 611 - 612, pp.844-851, 2014. DOI: 10.4028/www.scientific.net/KEM.611-612.844

[9] Venkateswaran G., Cameron M.R., Jabarin S.A. Effects of temperature profiles through preform thickness on the properties of reheat-blown PET containers. Adv. Polym. Technol., 17 (3) (1998), pp. 237-249, 10.1002/(SICI)1098-2329(199823)17:3

[10] Y. M. Luo, L. Chevalier, F. Utheza, X. Nicolas. Simplified modeling of the convection and radiation heat transfers during the infrared heating of PET sheets and preforms Nomenclature. International Polymer Processing, 2015, 30 (5), pp.554-565. https://doi.org/10.3139/217.3092

[11] Z.q. Yang, W. Naeem, G. Menary, J. Deng, K. Li. (2014). Advanced Modelling and Optimization of Infared Oven in Injection Stretch Blow-moulding for Energy Saving, IFAC Proceedings Volumes, Volume 47, Issue 3, Pages 766-771, ISSN 1474-6670, https://doi.org/10.3182/20140824-6-ZA-1003.01191

[12] M. Bordival, F. M. Schmidt, Y. Le Maoult and V. Velay. (2009). Optimisation of preform temperature distribution for the stretch-blow moulding of PET bottles: Infrared heating and blowing modelling, Polymer Engineering and Science, vol. 49, no. 4, pp. 783-793. DOI:10.1007/s12289-008-0232-8

[13] Z.q. Yang, W. Naeem, G. Menary, J. Deng, K. Li. (2014). Advanced Modelling and Optimization of Infared Oven in Injection Stretch Blow-moulding for Energy Saving, IFAC Proceedings Volumes, Volume 47, Issue 3, Pages 766-771, ISSN 1474-6670, https://doi.org/10.3182/20140824-6-ZA-1003.01191

[14] Nguyen, T.T., Luo, YM., Chevalier, L. et al. Numerical Simulation of Infrared Heating and Ventilation before Stretch Blow Molding of PET Bottles. Int J Mater Form 16, 37 (2023). https://doi.org/10.1007/s12289-023-01763-2

[15] Nixon J, Menary G. H., Yan S. (2017). Assessing the Stretch-blow Moulding FE Simulation of PET over a Large Process Window. AIP Conference Proceedings 1896, 060008; https://doi.org/10.1063/1.5008071